



## INFLUENCE OF RUTHENIUM ON STRUCTURAL, OPTICAL AND ELECTRICAL PROPERTIES OF V<sub>2</sub>O<sub>5</sub> THIN FILMS DEPOSITION AT DIFFERENT PERCENTAGES

A. Sherin Fathima<sup>1</sup>, I.Kartharinal Punithavthy<sup>1\*</sup>, S.Johnson Jeyakumar<sup>1</sup>,  
A. Rajeshwari, A. Sindhya

<sup>1</sup>Department of Physics, T.B.M.L College (Affiliated to Bharathidasan University, Trichy),  
Porayar, Tamil Nadu - 609307, India.

\*Corresponding Author: [profpunithaphysics@gmail.com](mailto:profpunithaphysics@gmail.com)

### Abstract

Nowadays, semiconducting thin films are efficient candidates for good optical and electrical properties. In this present study, thin films of Ruthenium (Ru) doped V<sub>2</sub>O<sub>5</sub> with different weight percentages were prepared through the method of spray Pyrolysis. The prepared Ru doped thin films were characterized by spectrographic tools such as XRD, SEM with EDAX, FT-IR, UV-vis and Hall effect to study their crystalline nature, functional group, band gap, resistivity, conductivity and mobility of the flow of electrons respectively. The structural morphology of the synthesized thin films was discussed through the micrographic image obtained from Scanning electron microscopy together with their surface occupancy plots. The obtained minimum crystallite size is about 24.8 nm for 8% molarities. The morphological and structural studies show enhanced results for an 8% sample which makes it a viable candidate for optical and electrical applications.

**Keywords:** Spray Pyrolysis, V<sub>2</sub>O<sub>5</sub> Thin films, Surface Morphology, Ruthenium, and Electrical Properties.

### 1.Introduction

Nowadays, thin films of V<sub>2</sub>O<sub>5</sub> have gained noteworthy attention in the microelectronic world [1]. In recent years, vanadium oxides play a vital role due to their sensing activity, selective catalytic and potential applications in electrochemical capacitors [2-5]. And also, vanadium oxide thin film has a scientific and technological application which includes electrochromic devices (ECD), toxic gas detectors, electronic and optical switches [6-8]. Vanadium oxides have interesting electronic structures is 3d<sup>3</sup>4s<sup>2</sup> electrons in their outer shell, which enables them to be in different oxidation states such as V<sup>2+</sup>, V<sup>3+</sup>, V<sup>4+</sup> and V<sup>5+</sup>. This creates complex as well as challenging material. In different vanadium oxides, vanadium pentoxide (V<sub>2</sub>O<sub>5</sub>) is widely used and is stable. The direct band gap of V<sub>2</sub>O<sub>5</sub> makes V<sub>2</sub>O<sub>5</sub> thin films lay footprints in photodetection applications which leads to the utilizing V<sub>2</sub>O<sub>5</sub> thin films

in optoelectronic devices [9]. However, pure crystalline V<sub>2</sub>O<sub>5</sub> generally possess an orthorhombic structure that comprises better chemical property and good specific energy with thermal stability [10]. Because of the mentioned properties of V<sub>2</sub>O<sub>5</sub> crystal's orthorhombic structure, these V<sub>2</sub>O<sub>5</sub> thin films and their related materials were used for fabricating IR detectors, solar cells and sensors too.

V<sub>2</sub>O<sub>5</sub> thin film has been synthesized using various methods such as sputtering [11], sol-gel method [12], hydrothermal [13], pulsed laser deposition [14], chemical vapor deposition [15] and co-precipitation technique [16], etc. Among, these various deposition techniques, the thermal evaporation method is the most predominant. The thermal evaporation technique is the most challenging versatile method for the deposition of V<sub>2</sub>O<sub>5</sub> thin films.

However, High surface area V<sub>2</sub>O<sub>5</sub> aerogels exhibit a larger lithium intercalation capacity compared to crystalline V<sub>2</sub>O<sub>5</sub>. Hence, a major difficulty of these electrodes is their limited long-term cycling stability. To overcome the specific rate, intercalation rate and cycling performance of vanadium oxide metal such as M<sub>x</sub>V<sub>2</sub>O<sub>5</sub> (M= Zr, Ag, Ru, etc.) have been taken to be used as cathode materials due to their unique structure. Moreover, there is no report so far of V<sub>2</sub>O<sub>5</sub> particles doped by Ruthenium in lithium-ion batteries at high deposition temperatures. In the present work, pure and Ruthenium doped V<sub>2</sub>O<sub>5</sub> thin film in various molar percentages [2, 4, 6 and 8%] were deposited. These prepared thin films were synthesized by the spray pyrolysis technique.

The obtained pure and Ruthenium doped V<sub>2</sub>O<sub>5</sub> thin film were characterized by X-ray diffraction (XRD) for structural analysis, scanning electron microscope (SEM) was used to examine the surface morphology and the electrical studies hall effect were also recorded to find the conductivity of the prepared thin films.

## 2. Experimental Procedure

V<sub>2</sub>O<sub>5</sub> thin films were prepared onto ITO substrates by spray pyrolysis of pure V<sub>2</sub>O<sub>5</sub> powder from an electrically heated molybdenum boat kept at ~ 1823 K in a vacuum very good than 8 x 10<sup>-6</sup> Torr. A Hind High Vacuum 12A4 Coating was used for the deposition of the experimental thin films. A diffusion pump backed by a rotary pump was carried to produce the pressure of 3 x 10<sup>-6</sup> Torr. Well-Polished ITO substrates were mounted on a copper holder which was fixed on a tripod in the bell jar. After getting the ultimate vacuum of 5 x 10<sup>-6</sup> Torr and the desired substrate temperature in the chamber, the glow discharge was initiated further ionically polished the substrates in the vacuum chamber. This process was done for two minutes. The system was allowed to reach the ultimate vacuum so that the crystalline nature of Ru doped V<sub>2</sub>O<sub>5</sub> thin films can be enhanced. When the power was fed to the boat, the material in the boat evaporated and the vapors reacted with the oxygen gas leading to film deposition on the substrate. The temperature of the boat during deposition was monitored using an optical pyrometer [17]. The substrates were sustained at the required deposition temperature and the molybdenum boat in which Ruthenium (Ru) doped V<sub>2</sub>O<sub>5</sub> powder with different weight percentages kept. The shutter covering the substrates was opened when the required temperature of the boat reached about 1823 K and it was maintained during the deposition of

the films.

## 2.1 Characterization

The well-adherent V<sub>2</sub>O<sub>5</sub> films underwent structural, morphological and optical studies. The structural properties characterization by X-ray diffraction is carried out using X'Pert High Scorer-Panalytical Diffractometer with Cu-K radiation of wavelength ( $\lambda=1.5406\text{\AA}$ ). The morphology was analyzed by Scanning Electron Microscope (Hitachi S-4500 SEM machine). The spectroscopic vibration studies of Ru doped V<sub>2</sub>O<sub>5</sub> thin films have been performed on FT-IR (PerkinElmer L1600) between the wavenumber range of 400–4000 cm<sup>-1</sup>. The optical studies evolved using UV spectrophotometer, and the wavelength was prescribed from 200 to 800 nm. And the Electrical studies were carried out using the Hall Effect.

## 3. Result and Discussion

### 3.1 Structural Analysis

XRD patterns of pure and Ruthenium doped V<sub>2</sub>O<sub>5</sub> thin films with different weight percentages (2%, 4%, 6% and 8%) are shown in Fig. 1. The obtained thin films reveal characteristic peaks related to orthorhombic phase crystal structure. The noticed peaks are gently matched with standard patterns of JCPDS card No. 89-2482 and the peaks 20.85, 30.00, 34.97, 50.27, 55.02, and 59.80 at crystal plane (101), (012) and (312) respectively [18]. The crystallite size of the prepared Ru doped thin films was calculated using Debye's Scherrer formula [19],

$$D = \frac{K\lambda}{\beta \cos\theta} \quad \text{-----[1]}$$

Where K is a Scherrer constant,  $\lambda$  is the wavelength of the beam,  $\beta$  is (FWHM) and  $\theta$  is Bragg's diffraction angle. The average crystallite size of the prepared thin films decreases from 29.5 to 22.2nm with the increase in weight percentage, which is due to the different ionic radii of Ru and V<sub>2</sub>O<sub>5</sub>. Compared with the pure V<sub>2</sub>O<sub>5</sub>, the minute peaks disappeared, when increasing the weight percentage [20]. However, the average dislocation density and Average micro strain of the prepared thin films are increased linearly with the increase of weight percentages.

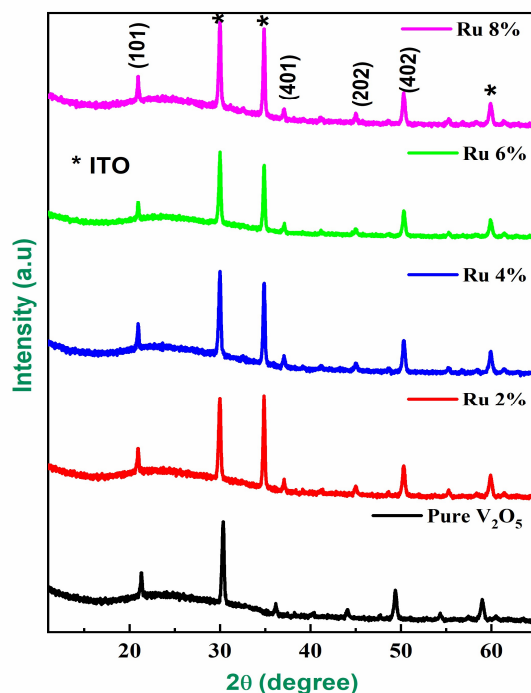


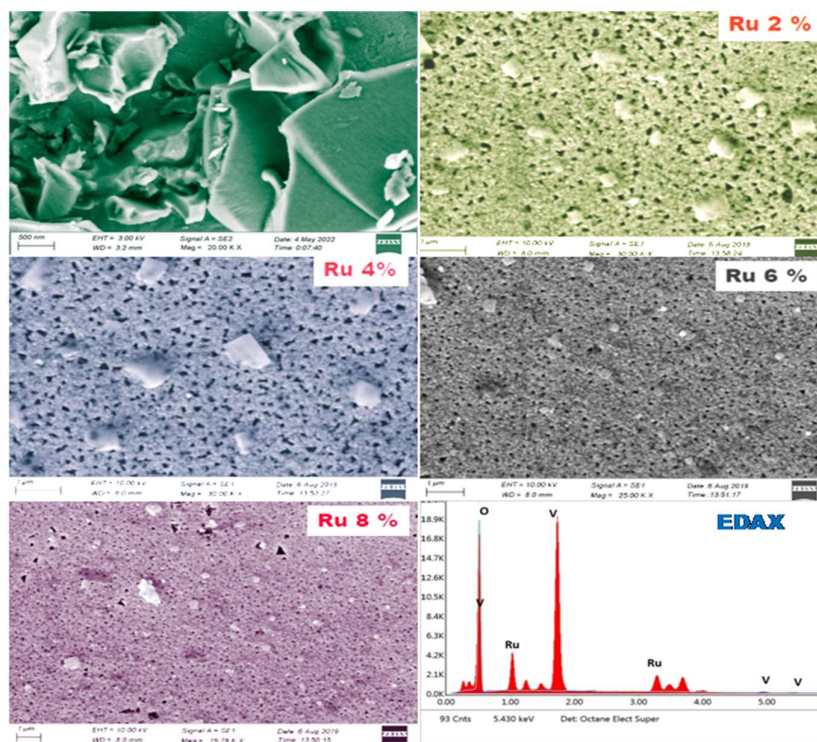
Fig. 1 XRD patterns of pure V<sub>2</sub>O<sub>5</sub> with different weight percentages

Table1. Structural parameters of pure V<sub>2</sub>O<sub>5</sub> with different weight percentages

S.No	Sample	Average crystallite size X10 <sup>-9</sup> m	Average Dislocation density X10 <sup>14</sup> m	Average Microstrain, ε X10 <sup>-3</sup> m
1	V <sub>2</sub> O <sub>5</sub>	29.5	1.14061E+15	0.00122
2	2%	28.3	1.2461E+15	0.00138
3	4%	26.8	1.38471E+15	0.00154
4	6%	24.6	1.52471E+15	0.00184
5	8%	22.2	1.65471E+15	0.00213

### 3.2 Morphology Studies

#### 3.2.1 SEM Micrographs



**Fig 2. SEM with EDAX images of Ru-doped  $V_2O_5$  with different weight percentages**

SEM images of Ru-doped  $V_2O_5$  with different weight percentages (2, 4, 6 and 8%) thin films are shown in Fig2. From the Figure the prepared thin films were spongy in shape with few agglomerations. The noticed spongy-like shape gets reduced in the increase of Ruthenium dopant percentage. The 8% Ru doped  $V_2O_5$  thin film shows a smooth surface with plateless scattered on its Surface. In Fig 2, EDAX shows the confirmation of occurred elements such as Ruthenium, vanadium, and oxide with their appropriate atomic ratio. There is no secondary phase of impurity.

### 3.2.2 Surface Occupancy plots

We intended to illustrate the surface micro structural condition of pure and varied percentages of Ruthenium iondoped  $V_2O_5$ films, as seen in the previous SEM photographs. Here, the surface condition was demonstrated with the aid of a surface occupancy plot through image J. Thin film samples have been shown in Fig 3(a-e) to illustrate the surface occupancy state. To begin, to compare the outcomes of the SEM compared with those of the SOP, in the case of pure  $V_2O_5$  thin film, the SEM reveals a peeled micro structural condition along with crippled and aggregated conditions, as shown in Fig. 3. The SOP reveals that the signals must be intensified in certain regions due to the microstructures' clumping. However, after incorporating 2%, 4% and 6% of Ru-ions into the  $V_2O_5$ , the surface morphology was radically transformed, as depicted in Fig.3(b-d), exhibiting pinholes – (micro channels) appearing in the scanning region. The mild, consistent signals with some strong signals due to minor agglomerations are visible in their SOP. After that, in the case of 8% of Ru-ion doped  $V_2O_5$



SOP having very smooth and well-distributed signals with a reduction in micro structural sizes, as seen in Fig. 3e. So, we infer that the current SOP study has appropriate evidence for the Ru-ions implications in host thin film. We suggest the vital thing about the pin-hole and void formations, which are acquired due to defects arising in crystalline V<sub>2</sub>O<sub>5</sub> while interrupting with dopant ions. As a result of the exterior diffusion of Ru-ions during specimen meets calcination in thin films, multiple stoichiometry vacancies can be created in this kind of cavity. The microstructural parameters in this instance of pin-holes are more advantageous for charge transfers, suggesting that they may operate as channels, resulting in improved electrical conductivity [21]. Ultimately based on the outcomes, it was found that various Ru-ions doped V<sub>2</sub>O<sub>5</sub> thin films were more useful for solar cell-based applications.

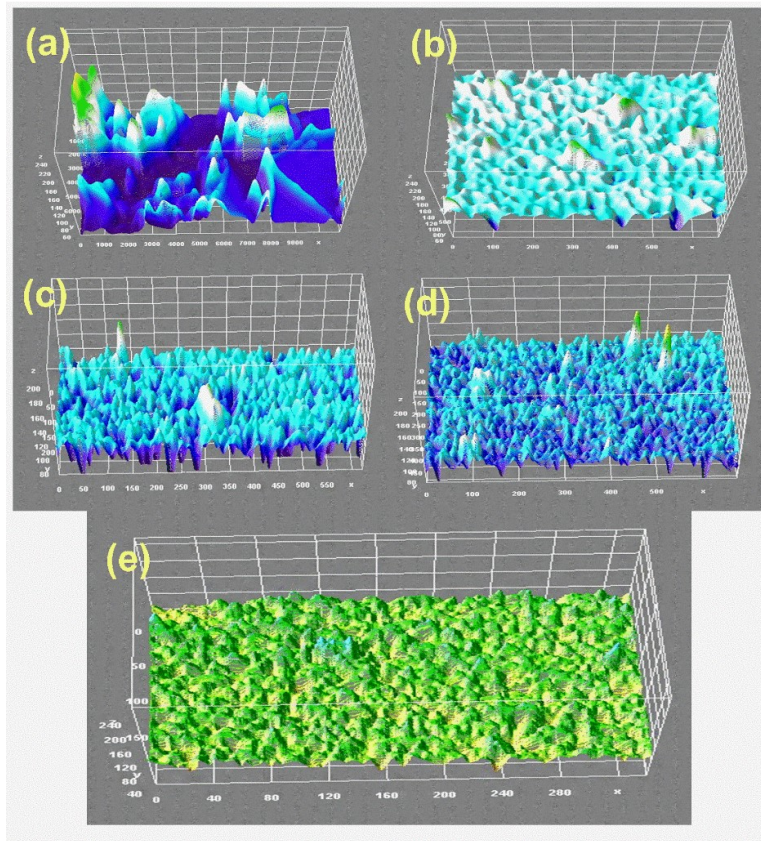


Fig. 3(a-e) Surface Occupancy plots of Ru-doped V<sub>2</sub>O<sub>5</sub> with different weight percentages

### 3.3 Functional Studies

Fig.4 depicts the FT-IR spectra of pure and varied percentages of Ruthenium ion-doped V<sub>2</sub>O<sub>5</sub> films. The presence of functional groups in the produced thin films are further confirmed by the absorption of IR in molecular vibrations. The stretching vibration of the metal-oxide bond is represented by the vibrational frequency at 621cm<sup>-1</sup>. Water molecules stretching vibration O-H bonds are responsible for the strong, intense peak at 3250 cm<sup>-1</sup>. O-H bending

vibration is responsible for the peak at  $1310\text{ cm}^{-1}$ , which is caused by the calcinated thermal interfaces, on the other hand, the experimental reaction may be a factor for O-H molecule incorporation[22].

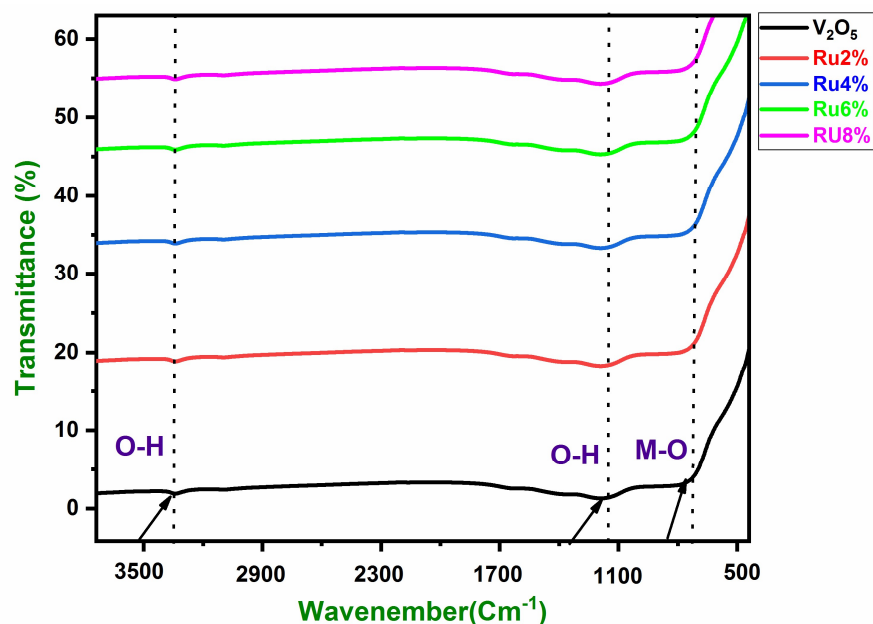


Fig.4 FTIR Spectra of Ru doped  $\text{V}_2\text{O}_5$  with different weight percentages

Table.2 FT-IR Spectra of Ru doped  $\text{V}_2\text{O}_5$  with different percentages

S.N	Vibrational assignments	Experimental absorption ( $\text{cm}^{-1}$ )				
		$\text{V}_2\text{O}_5$	2%	4%	6%	8%
1	Metal - oxide	621	621	621	621	621
2	O - H bending vibration	1310	1310	1310	1310	1310
3	O - H stretching vibration	3250	3250	3250	3250	3250

### 3.4 Optical Studies

Figure 5 depicts the UV-Vis spectra of Ruthenium ion-doped  $\text{V}_2\text{O}_5$  films with different weight percentages (2% to 8%). As the doping percentage rises, the absorbance decreases monotonously. The abrupt drops in transmittance are caused by the absorption of the majority of incoming photons with wavelengths between 300 nm and 800 nm. The region of fundamental absorption edge for ITO coated Ru doped  $\text{V}_2\text{O}_5$  thin films with absorbance values of 325.6, 320.8, 317.4, 311.1 and 305.4 at 2% to 8% are depicted in Fig.5. The spectra show that the absorption edge indicates a red shift in wavelength as crystallite size decreases, which suggests a shift on the lower energy side. The microstructure and growth conditions of the films have an impact

on the optical characteristics of ITO-coated Ru-doped V<sub>2</sub>O<sub>5</sub> thin films with various weight percentages.

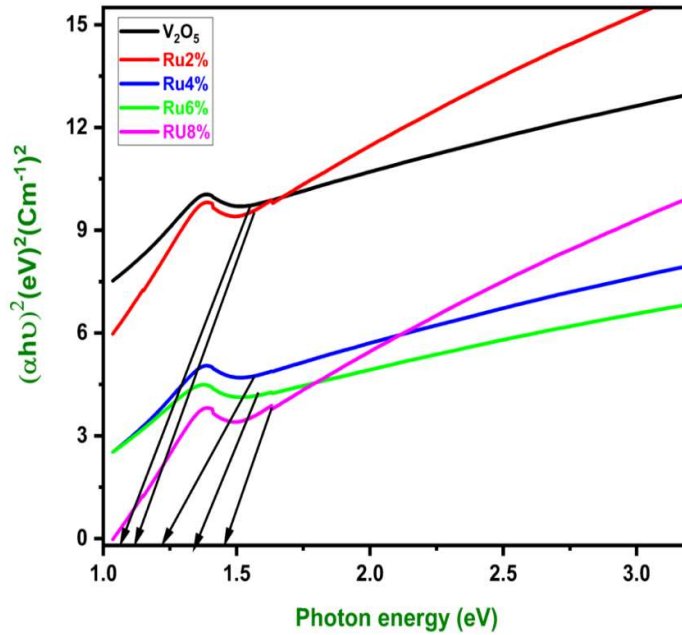


**Fig. 5 Optical absorption spectra of Ru-doped V<sub>2</sub>O<sub>5</sub> with different percentages**

The optical band gap energies are 2.06, 2.11, 2.16, 2.28, and 2.39 eV. The band gap energies are increases with the increase in doping percentage which is agreed with the Brus equation [23]. Furthermore, the widening of bandgap in the prepared Rudoped V<sub>2</sub>O<sub>5</sub> thin films is due to the phenomenon of quantum size effects, which is higher for films at low growth temperatures, where the size of grains is relatively low ( $\leq 50\text{nm}$ ). In addition, the mean crystal dimension becomes small; therefore, the quantum size effects lead to increase in the band gap. The defects in the lattice of Ru-doped V<sub>2</sub>O<sub>5</sub> thin films are due to the oxygen vacancy between two V-O layers that create lower absorption bands in optical spectra. This oxygen vacancy is raised due to the disorders inatomic arrangement.



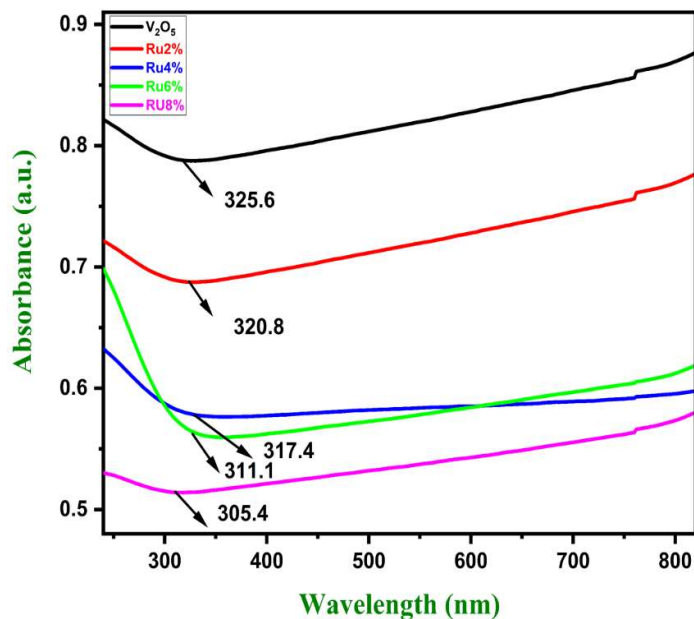


Fig. 6 Bandgap energy of Ru-doped V<sub>2</sub>O<sub>5</sub> with different percentages

Table.3 Optical properties of Rudoped V<sub>2</sub>O<sub>5</sub> with different percentages

Composition	Absorbance	Bandgap (eV)
V <sub>2</sub> O <sub>5</sub>	325.6	2.06
2%	320.8	2.11
4%	317.4	2.16
6%	311.1	2.28
8%	305.4	2.39

### 3.5 Electrical Studies

#### 3.5.1 Hall Effect

The transport parameters of the prepared samples were studied by using the Hall Effect at room temperature. The changes in the electrical transport because of increasing the dopant amount of Ruthenium in V<sub>2</sub>O<sub>5</sub> thin films are summarized in the Table.4. The ions of vanadium show semiconducting features because of their different oxidation states due to the bouncing of 3d unpaired electrons. Fig. 7(a) shows the mobility and carrier concentration of the pure V<sub>2</sub>O<sub>5</sub> thin films and V<sub>2</sub>O<sub>5</sub> thin films doped with (2,4,6 and 8%) of ruthenium. It shows that the mobility and carrier concentration increases for 2% of dopants and then it gradually decreases for 4,6 and 8% of dopants.

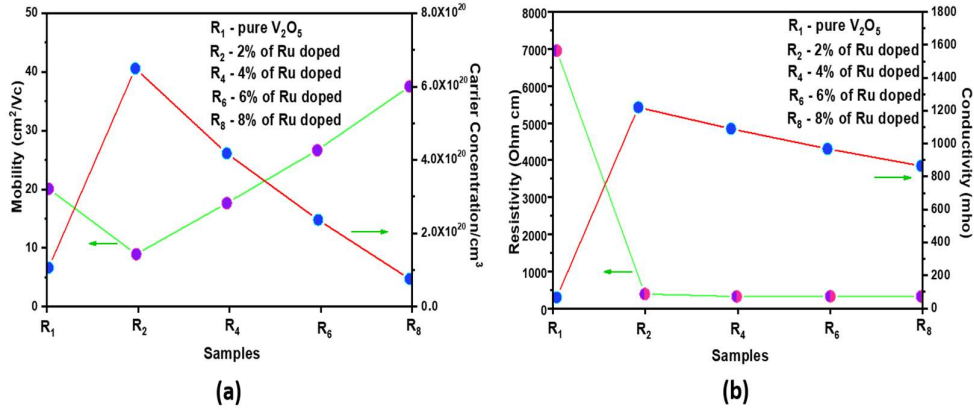


**Fig. 7** Electrical studies of V<sub>2</sub>O<sub>5</sub> thin films with different percentages

However, Fig.7(b) shows the resistivity and conductivity of the pure V<sub>2</sub>O<sub>5</sub> thin films and V<sub>2</sub>O<sub>5</sub> thin films doped with (2, 4, 6 and 8%) of Ruthenium. which portrays that, the thin film's conductivity rises as a result of the creation of Oxygen vacancies. So, the Ruthenium inclusion on the V<sub>2</sub>O<sub>5</sub> thin film matrix leads to a remarkable influence on the mobility of the prepared samples is revealed.

**Table.4** Electrical parameters of V<sub>2</sub>O<sub>5</sub> thin films with different percentages

Sample	Resistivity (ρ)(Ω cm)	Conductivity (σ)(Ω cm) <sup>-1</sup>	Mobility (μ)(cm <sup>2</sup> /Vs)	Carrier concentration/C m <sup>3</sup>
R <sub>0</sub>	2.19x10 <sup>3</sup>	4.61x10 <sup>2</sup>	0.8 x10 <sup>1</sup>	1.7 x10 <sup>20</sup>
R <sub>2</sub>	6.45x10 <sup>3</sup>	1.17 x10 <sup>2</sup>	4 x10 <sup>1</sup>	6.8 x10 <sup>20</sup>
R <sub>4</sub>	4.89x10 <sup>3</sup>	1.09 x10 <sup>2</sup>	2.5 x10 <sup>1</sup>	4.4x10 <sup>20</sup>
R <sub>6</sub>	4.39 x10 <sup>3</sup>	0.95 x10 <sup>2</sup>	1.4 x10 <sup>1</sup>	2.5x10 <sup>20</sup>
R <sub>8</sub>	3.97 x10 <sup>3</sup>	0.88 x10 <sup>2</sup>	0.45 x10 <sup>1</sup>	0.8x10 <sup>20</sup>

#### 4. Conclusion

The thin films of Pure V<sub>2</sub>O<sub>5</sub> with different weight percentages (2, 4, 6 and 8%) were prepared and coated in the ITO substrate by the method of spray pyrolysis. The XRD pattern shows the respective peaks of the prepared V<sub>2</sub>O<sub>5</sub> thin films with orthorhombic structures. The average crystallite size of the Pure V<sub>2</sub>O<sub>5</sub> and doped Ruthenium with different weight percentages are 29.5 to 22.2 nm respectively. It shows that the crystallite size decreases with the increase in weight percentages. The FTIR spectra show the appropriate bands of bonds present in the prepared samples, while the optical spectra show their corresponding absorption spectra with their respective band gaps, which indirectly shows the prepared material is a semiconductor. In addition, the SEM/EDAX micrographs show that the synthesized thin films were formed in the shape of crumbled paper for 8% of molar concentration. However, surface occupancy plots show that sheet-like particles are uniformly distributed over the scanning

surface area. Hence, this present study suggests that  $V_2O_5$  thin films prepared through spray pyrolysis with the increase in the dopant weight percentages enhance its optical and electrical properties, which may lead to use the prepared samples for effective optical and electrical applications.

### Compliance with ethical standards

**Conflict of interest:** The authors declare that they have no conflict of interest

### References

1. Xia, Qiuying, Feng Zan, Jing Xu, Wei Liu, Qichanghao Li, Yan He, Jingyi Hua et al. "All-Solid-State Thin Film Lithium/Lithium-Ion Microbatteries for Powering the Internet of Things." *Advanced Materials* (2022): 2200538.
2. Theerthagiri, Jayaraman, Govindarajan Durai, K. Karuppasamy, Prabhakarn Arunachalam, Venugopal Elakkiya, Parasuraman Kuppasami, Thandavarayan Maiyalagan, and Hyun-Seok Kim. "Recent advances in 2-D nanostructured metal nitrides, carbides, and phosphides electrodes for electrochemical supercapacitors—a brief review." *Journal of Industrial and Engineering Chemistry* 67 (2018): 12-27.
3. Mirzaeian, Mojtaba, Nazym Akhanova, Maratbek Gabdullin, Zhanar Kalkozova, Aida Tulegenova, Shyryn Nurbolat, and Khabibulla Abdullin. "Improvement of the pseudocapacitive performance of cobalt oxide-based electrodes for electrochemical capacitors." *Energies* 13, no. 19 (2020): 5228.
4. Xue, Yudong, and Yunting Wang. "A review of the  $\alpha$ -Fe<sub>2</sub>O<sub>3</sub> (hematite) nanotube structure: recent advances in synthesis, characterization, and applications." *Nanoscale* 12, no. 20 (2020): 10912-10932.
5. Lu, Xiaofeng, Wanjin Zhang, Ce Wang, Ten-Chin Wen, and Yen Wei. "One-dimensional conducting polymer nanocomposites: Synthesis, properties and applications." *Progress in Polymer Science* 36, no. 5 (2011): 671-712.
6. Le, Top Khac, Phuong V. Pham, Chung-Li Dong, Naoufal Bahlawane, Dimitra Vernadou, Issam Mejri, Aline Rougier, and Sok Won Kim. "Recent Advances in Vanadium Pentoxide ( $V_2O_5$ ) Towards Related Applications on Chromogenic and Beyond: Fundamentals, Progress, and Perspectives." *Journal of Materials Chemistry C* (2022).
7. Gok, Elif Ceren, Murat Onur Yildirim, Esin Eren, and Aysegul Uygun Oksuz. "Comparison of Machine Learning Models on Performance of Single- and Dual-Type Electrochromic Devices." *ACS omega* 5, no. 36 (2020): 23257-23267.
8. Zhou, Lan, Qimin Yan, Aniketa Shinde, Dan Guevarra, Paul F. Newhouse, Natalie Becerra-Stasiewicz, Shawn M. Chatman, Joel A. Haber, Jeffrey B. Neaton, and John M. Gregoire. "High throughput discovery of solar fuels photoanodes in the CuO- $V_2O_5$  system." *Advanced Energy Materials* 5, no. 22 (2015): 1500968.
9. Kianfar, Ehsan. "Recent advances in synthesis, properties, and applications of vanadium oxide nanotube." *Microchemical Journal* 145 (2019): 966-978.

10. Navone, C., Rita Baddour-Hadjean, J. P. Pereira-Ramos, and R. Salot. "High-performance oriented V2O5 thin films prepared by DC sputtering for rechargeable lithium microbatteries." *Journal of the Electrochemical Society* 152, no. 9 (2005): A1790.
11. Raj, D. Vasanth, N. Ponpandian, D. Mangalaraj, and C. Viswanathan. "Effect of annealing and electrochemical properties of sol-gel dip coated nanocrystalline V2O5 thin films." *Materials Science in Semiconductor Processing* 16, no. 2 (2013): 256-262.
12. Margoni, Mudaliar Mahesh, S. Mathuri, K. Ramamurthi, R. Ramesh Babu, V. Ganesh, and K. Sethuraman. "Hydrothermally grown nano and microstructured V2O5 thin films for electrochromic application." *Applied Surface Science* 449 (2018): 193-202.
13. Beke, Structural, Sl Giorgio, L. Körösi, L. Nanai, and W. Marine. "Structural and optical properties of pulsed laser deposited V2O5 thin films." *Thin Solid Films* 516, no. 15 (2008): 4659-4664.
14. Nandakumar, Navaneetha Krishnan, and Edmund G. Seebauer. "Low temperature chemical vapor deposition of nanocrystalline V2O5 thin films." *Thin Solid Films* 519, no. 11 (2011): 3663-3668.
15. Rosaiah, P., G. Lakshmi Sandhya, and O. M. Hussain. "Impedance spectroscopy and electrochemical properties of nano-crystalline vanadium pentoxide (V2O5) synthesized by co-precipitation method." *Advanced Science, Engineering and Medicine* 8, no. 2 (2016): 83-90.
16. Ho, Soon Min, Vanalakar SA, Galal Ahmed, and Nand Singh Vidya. "A review of nanostructured thin films for gas sensing and corrosion protection." *Mediterranean Journal of Chemistry* 7, no. 6 (2018).
17. Nandhini, S., N. Maheswari, and G. Muralidharan. "Electrochemical behavior of novel  $\beta$ -Mn3O4/V2O5 electrode using gel electrolyte for high performance supercapacitors." In *AIP Conference Proceedings*, vol. 1832, no. 1, p. 050040. AIP Publishing LLC, 2017.
18. Al-Zaqri, Nabil, K. Umamakshvari, V. Mohana, A. Muthuvel, and Ahmed Boshala. "Green synthesis of nickel oxide nanoparticles and its photocatalytic degradation and antibacterial activity." *Journal of Materials Science: Materials in Electronics* 33, no. 15 (2022): 11864-11880.
19. Cao, Huili, Zhiyong Zheng, Poul Norby, Xinxin Xiao, and Susanne Mossin. "Electrochemically Induced Phase Transition in V3O7·H2O Nanobelts/Reduced Graphene Oxide Composites for Aqueous Zinc-Ion Batteries." *Small* 17, no. 24 (2021): 2100558.
20. Park, Sangsik, Seung Hyun Kim, Hyun Ho Choi, Boseok Kang, and Kilwon Cho. "Recent advances in the bias stress stability of organic transistors." *Advanced Functional Materials* 30, no. 20 (2020): 1904590.
21. Bombelli, Paolo, Marie Zarrouati, Rebecca J. Thorne, Kenneth Schneider, Stephen JL Rowden, Akin Ali, Kamran Yunus et al. "Surface morphology and surface energy of anode materials influence power outputs in a multi-channel mediatorless biophotovoltaic (BPV) system." *Physical Chemistry Chemical Physics* 14, no. 35 (2012): 12221-12229.

22. Yang, Jinhui, and Xiaogang Luo. "Ag-doped TiO<sub>2</sub> immobilized cellulose-derived carbon beads: One-Pot preparation, photocatalytic degradation performance and mechanism of ceftriaxone sodium." *Applied Surface Science* 542 (2021): 148724.
23. Vasudevan, J., S. Johnson Jeyakumar, B. Arunkumar, M. Jothibas, A. Muthuvel, and S. Vijayalakshmi. "Optical and magnetic investigation of Cu doped ZnO nanoparticles synthesized by solid state method." *Materials Today: Proceedings* 48 (2022): 438-442.